Crystal Structure and Growth Behavior of Aspartame Form I-A

ARTICLE *in* CRYSTAL GROWTH & DESIGN · MAY 2005

Impact Factor: 4.89 · DOI: 10.1021/cg049676m

8 AUTHORS, INCLUDING:

Rene de Gelder
Radboud University Nijmegen
211 PUBLICATIONS **2,808** CITATIONS
SEE PROFILE

Reinier F. P. Grimbergen
Royal DSM
28 PUBLICATIONS **444** CITATIONS
SEE PROFILE

CRYSTAL GROWTH & DESIGN
2005
VOL. 5, NO. 3
917−923

Crystal Structure and Growth Behavior of Aspartame Form I-A

H. M. Cuppen,[†,||] G. Beurskens,[‡] S. Kozuka,[§] K. Tsukamoto,[§] J. M. M. Smits,[‡] R. de Gelder,[‡] R. F. P. Grimbergen,[#] and H. Meekes*,[†]

IMM Department of Solid State Chemistry, Radboud University Nijmegen, Toernooiveld 1, 6525 ED Nijmegen, The Netherlands, IMM Department of Chemical Crystallography, Radboud University Nijmegen, Toernooiveld 1, 6525 ED Nijmegen, The Netherlands, Graduate School for Science, Tohuku University, Aramaki, Aoba, 980-8578 Sendai, Japan, and DSM Composite Resins, P.O. Box 615, 8000 AP Zwolle, The Netherlands

Received September 24, 2004; Revised Manuscript Received January 4, 2005

ABSTRACT: The structure, morphology, and growth behavior of aspartame form I-A are presented. This form can be obtained from a purely aqueous solution and is the form with the highest industrial importance. The aspartame molecules are arranged around large hydrophilic channels filled with water molecules. The crystal morphology of this compound is needlelike with polar growth behavior in the needle direction. The side faces show a large nucleation barrier for growth, whereas the top faces possess a much smaller barrier. Monte Carlo simulations are performed for this crystal structure, and the resulting growth rate, morphology, and polarity are all in agreement with the experimental observations.

Introduction

Aspartame is an artificial low-calorie sweetener, 200 times sweeter than sugar, and is as such an important component in many low-calorie, sugar-free foods and drinks. The molecule consists of two amino acids: L-phenylalanine and L-aspartic acid giving aspartame a hydrophobic and a hydrophilic side. Aspartame is known to grow in different pseudo-polymorphic forms, each containing a different amount of water of hydration and all having a needlelike morphology. All forms generally give rise to spherulites consisting of very fine needles. Only for one polymorph, form II-A, is the complete crystal structure reported in the Cambridge Structural Database (CSD).[1] Form II-A can only be obtained from a solvent mixture and not from a purely aqueous solution and is as such of less industrial importance. In a previous paper,[2] the needle morphology with a very high aspect ratio was explained in detail for this form using Monte Carlo simulations for the growth rates of the crystal faces. The relatively high growth rate of the faces that determine the needle tops turned out to be due to unexpectedly small values for the edge energies of steps on these faces. The high symmetry of form II-A results in a canceling of many bond energies that determine the step energies. In contrast with form II-A, form I-A can be obtained from a purely aqueous solution and is the pseudo-polymorph that is generally produced in the manufacturing process of aspartame. Form I-A was known to have a lower spacegroup symmetry, although the structure was not determined.[3] This led to the question of whether the fine needle morphology of form I-A could still be explained by a canceling of bonds. The present paper highlights the structure of this form and its crystal morphology and growth behavior. The data obtained by computer simulations will be compared with experimental results.

Crystal Structure

Because of the extreme aspect ratio in pure water, leading to very thin needles, a single crystal X-ray structure determination is not straightforward. To obtain sufficiently thick crystals, various solvents were tried. The best results were obtained using a glycol−water mixture (28−72 mass %) resulting in needles with a thickness of 140−200 μm. Such a crystal was mounted in a glass capillary to ensure a constant water of hydration content. Intensity data were collected at room temperature on an Enraf-Nonius CAD4 single-crystal diffractometer, using Cu−Kα radiation and a $\omega - 2\theta$ scan mode. Unit cell dimensions were determined from the angular setting of 22 reflections. Intensity data were corrected for Lorentz and polarization effects. A semiempirical absorption correction (ψ scans)[4] was applied. Direct methods failed to solve the structure, probably because of the poor quality of the data and the lack of resolution. Patterson search methods, using the ORIENT and TRACOR programs from the DIRDIF program system,[5] were applied and were eventually successful. As the aspartame molecule does not contain a sufficiently large rigid fragment, two strategies were considered. In the first strategy, a fragment with three rotational degrees of freedom was used and about 200 conformations were generated and subjected to an automatic Patterson search. Unfortunately, none of them led to the solution of the structure, probably since the first orientation given by ORIENT and the first position given by TRACOR (which are only used in an automatic run) did not correspond to the correct solution. The solution could, however, be somewhere among the second or third peaks of the ORIENT and/or

|| Present address: 1012 Smith Lab, Ohio State University, Columbus, Ohio 43212.
* Corresponding author. Tel.: +31-24-365-32-00; fax: +31-24-365-30-67; e-mail: Hugo.Meekes@science.ru.nl.
† IMM Department of Solid State Chemistry, Radboud University Nijmegen.-
‡ IMM Department of Chemical Crystallography, Radboud University Nijmegen.
§ Tohuku University.
# DSM Composite Resins.

10.1021/cg049676m CCC: $30.25
Published on Web 02/17/2005

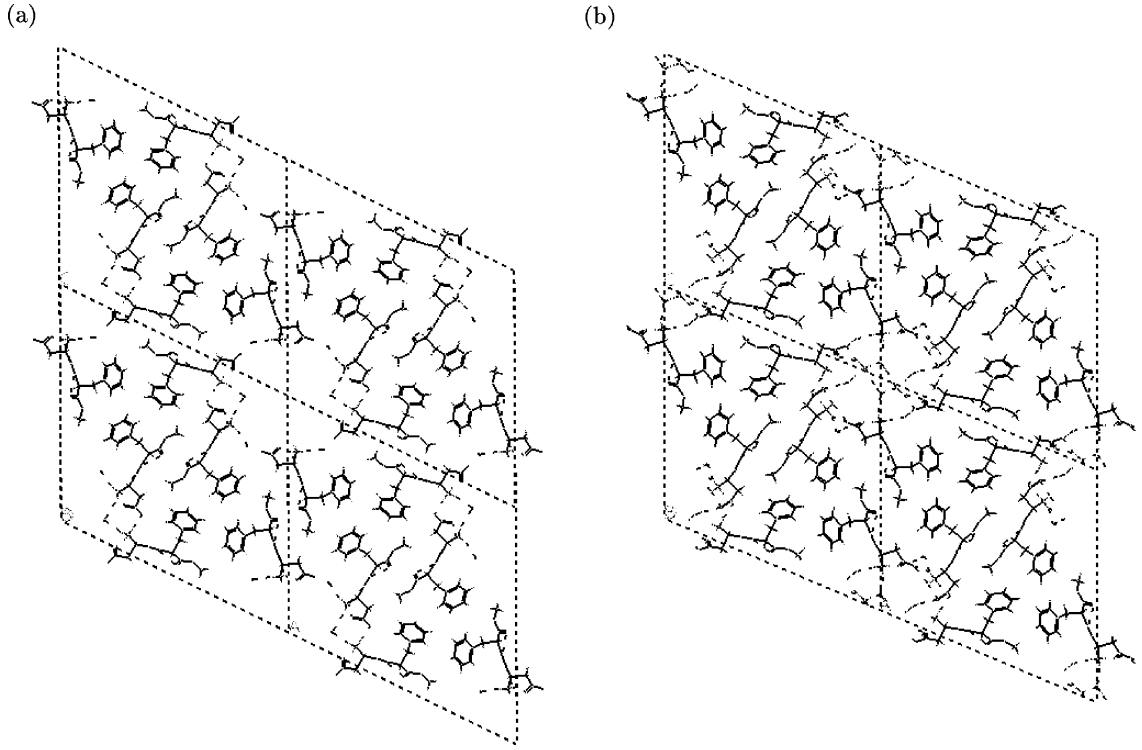

Figure 1. (a) *b*-projection of four unit cells of aspartame I-A; the hydrophilic channels are at the corners of the unit cell. The dashed lines indicate the hydrogen bonding. (b) The unit cell after minimization with 10 water molecules present. The molecules form a new hydrogen-bonding network.

TRACOR maps, but this was not analyzed any further. Thereafter, a second strategy was considered. Because of the similarity between the lengths of the very short unique axes of form II-A and the present form (present: $b = 4.880$ Å; form II-A: $c = 4.919$ Å[6]), the geometry of the aspartame molecule in form II-A served as a model in the orientation and translation search. This again did not lead to the solution of the structure. However, when the orientation of the five highest peaks in the search map were plotted, it was noticed that three of them represented molecules in orientations that were in rather good agreement with the orientations of the molecules in form II-A, which are arranged around a 4-fold axis (with almost no overlap in the *c*-direction). Each of the three orientations was subjected to a translation search, and one of the searches gave a distinctly higher peak. After we applied the corresponding shift and carefully expanded the structure with PHASEX, the structure was solved. The structure was further refined with standard methods (refinement against F^2 of all reflections with SHELXL97[7]) with anisotropic parameters for the non-hydrogen atoms. The hydrogens attached to the methyl groups were refined as rigid rotors to match maximum electron density in a difference Fourier map. All other hydrogens were placed at calculated positions and were refined riding on the parent atoms. The cell parameters are given in Table 1 together with the results found for form I-A by Meguro et al.[3] and the data for form II-A. The results are in accordance with the results found by Meguro et al. Figure 1a shows the projection along the *b* axis. Although the crystals of form I-A contain some 10.6 water molecules per unit cell,[12] only six of these are mentioned in Table 1 and in the deposited CCDC data. These six molecules are at well-defined positions in the skeleton that defines the channels of the crystal structure (see Figure 1a). The remaining 4−5 water molecules (the amount can vary within certain limits before the crystals attain another pseudo-polymorhic form) are inside the channels and are disordered as they are much more loosely bound to the skeleton. The large *R*-value is mainly due to the ill-defined positions of these water molecules. In these columns, there was scattered residual electron density, even after the final refinement, that was not attributed to atomic positions.

Table 1. Crystal Data for Aspartame Forms I-A and II-A[a]

	CSD-IA (250097)	CSD-IA (EFIFOO)	CSD-IIA (DAWGOX)
spacegroup	$P2_1$	$P2_1$	$P4_1$
a (Å)	25.450(2)	25.434	17.69
b (Å)	4.8795(9)	4.885	17.69
c (Å)	23.749(2)	23.776	4.92
α (°)	90	90	90
β (°)	116.468(8)	116.37	90
γ (°)	90	90	90
volume (Å^3)	2640.1(6)	2646.7	1538.5
density (Mg/m^3)	1.224		1.310
no. aspartame mol	6		4
no. water mol	6		2
final R1 [$I > 2\sigma(I)$]	0.1261		0.045
wR2 (all data)	0.3162		

[a] The second column gives the results of the present refinement; the third column the unit cell from XRPD data;[3] in the fourth column the single crystal data for form II-A[1] are added for comparison.

Experimental Section

The growth rate and morphology of aspartame form I-A were experimentally determined. For this purpose, saturated solutions in pure water at 40, 50, 60, and 70 °C were prepared.

Each solution was seeded with a needle crystal and fed to a sealed growth cell. The seed crystals were selected from spherulitic crystals, which were obtained by lowering the solution temperature without any agitation in a glass vessel. At low driving forces, faceted side faces were observed; at high driving forces, these faces became rounded. The seed crystals were placed into a slightly undersaturated solution before the growth experiment, followed by a gradual decrease of the solution temperature to achieve the desired driving force. The temperature of the solution was controlled with an accuracy of 0.1 K. The needles were observed with an optical microscope connected to a CCD camera during growth. The growth rate along the axial and the perpendicular directions were measured from the video images by employing image processing techniques.

Deposition number CCDC 250097 contains the supplementary crystallographic data for this paper. These data can be obtained free of charge via www.ccdc.cam.ac.uk/data_request/cif, by e-mailing data_request@ccdc.cam.ac.uk, or by contacting The Cambridge Crystallographic Data Centre, 12, Union Road, Cambridge CB2 1EZ, UK; fax: +44 1223 336033.

Monte Carlo Method

The simulation program MONTY[8] was used for all Monte Carlo simulations. MONTY is able to simulate the growth of any crystal surface at any temperature and driving force. The program uses a crystal graph of the crystal structure as input. We refer to Boerrigter et al.[8] for more details on the program. Monte Carlo simulations were performed for all faces parallel to at least one connected net. A simulation temperature of 300 K was used and simulation arrays of 50 × 50 unit cells, which corresponds to 15 000 molecules per layer. Periodic boundary conditions were applied to reduce edge effects.

For the attachment and detachment probabilities of the growth units the random rain scheme,[9,10] without surface diffusion, was used. The growth mechanism was 2D nucleation. Every simulation was preceded by a relaxation step of 3×10^6 cycles followed by a simulation of 10^7 cycles. During the simulations, we measured the growth rate R every 2×10^4 cycles. The growth rate is defined as

$$R = I_0 P^+ V_{\text{cell}} \text{SF} \tag{1}$$

where I_0 is the incoming flux of growth units per square meter per second, which is assumed to be constant, P^+ is the attachment probability, which is proportional to $\exp(\Delta\mu/kT)$, and V_{cell} is the volume of the unit cell. The sticking fraction SF is defined as

$$\text{SF} = \frac{\#\text{attachments} - \#\text{detachments}}{\#\text{attachments}} \tag{2}$$

Crystal Graph Representation

The Monte Carlo simulation program uses a crystal graph. In a crystal graph, the growth units are represented by dots and the intermolecular interactions between the growth units are represented by sticks with a certain bond strength. As we have no indication for the formation of dimers or other forms of clustering in the solution, we assume that the growth units are the aspartame molecules. The bond strengths are a summation of all individual interactions between the atoms in adjacent molecules. The construction of such a crystal graph is usually straightforward, provided that one has a reliable force field. For a detailed explanation of how to construct such a graph, we refer to Grimbergen et al.[11] In the case of aspartame, the procedure is more complicated, since the structure contains water.

Table 2. The Cell Parameters after Minimization of Aspartame I-A with the Presence of Water of Hydration and the Labels and Positions of the Centers of Gravity of the Four Aspartame Molecules in the Unit Cell

	a (Å)	b (Å)	c (Å)
	23.71	5.15	23.43
	α (°)	β (°)	γ (°)
	90.0	113.0	90.0
label	x	y	z
1	0.32	0.95	0.41
2	0.92	0.94	0.30
3	0.56	0.68	0.89
4	0.68	0.45	0.59
5	0.08	0.44	0.70
6	0.44	0.18	0.11

The problem when constructing a crystal graph is whether the water molecules play an important role in the stabilization of the crystal structure and whether the incorporation of the water molecules is the rate-limiting step. In the previous paper[2] for form II-A, it was argued that the water molecules do not play an important role in the hydrogen-bonding network and that the incorporation of the water molecules is not the rate-limiting step for crystal growth. For form II-A, the hydrophilic channel is bound by a ring of four aspartic groups of the aspartame molecules that are interconnected via hydrogen bonds. The water molecules in the structure form some additional hydrogen bonds within the channel. In the case of form I-A, the hydrophilic channel is made up of both water and aspartame molecules. Figure 1a indicates the hydrogen bonds by the dashed lines. Leaving the water molecules out during minimization would result in a deformation of the channel.

The crystal structure was therefore optimized with water molecules present while imposing the spacegroup symmetry of the structure. According to ref 12, the aspartame I-A structure contains 9.8 wt % water, which corresponds to 10.6 water molecules in the unit cell. We included 10 water molecules, which is four more than obtained from the crystal structure determination. Before optimization of the whole crystal structure, first the water molecules were optimized with all other parameters fixed. For all energy calculations, Cerius[2] with the Dreiding force field[13] in combination with ESP-derived point charges was used. Ewald summation was used during minimization. Table 2 shows the final lattice parameters and the positions and the labels of the centers of mass of the six aspartame growth units (GU) in the unit cell, and Figure 1b presents the optimized structure. This figure shows that the hydrophilic channel remained approximately the same and that the four additional water molecules are at the center of the channel bridging it via some hydrogen bonds. The lattice parameters in Tables 1 and 2 show that the force field leaves the structure reasonably the same.

The Monte Carlo simulations are performed to simulate the incorporation of molecules into the crystal. We therefore need to have some idea about the incorporation rate of the water molecules as compared to the

aspartame molecules. For the II-A structure, we saw that the water molecules are loosely bound in the hydrophilic channel and can probably move freely through the channel, although it is rather small. Since water is abundantly present in the system as a solvent, the water molecules were not included in the crystal graph used for the Monte Carlo simulations. Since form I-A has a larger water channel than the II-A structure and even more water is present in the system, the water molecules will probably move even more freely in the I-A structure. We therefore, again, did not include the water molecules in our crystal graph, by simply removing them from the structure optimized with the water molecules present.

All molecule−molecule interactions were then calculated in a range of three unit cells. The crystal graph was limited to the strongest interactions. The strongest interaction which was not included in the crystal graph has a strength of −9.41 kJ/mol. These bond energies were calculated with respect to a vacuum. Since our aim is to simulate the growth of aspartame from solution, we scaled the vacuum crystallization energy to the dissolution enthalpy. The dissolution enthalpy (ΔH = 35.1 kJ/mol) of phase I-A is used.[14] The scaling is achieved by setting the parameter E^{moth} in the Monte Carlo simulation program to −220.8 kJ/mol.[8] This parameter scales the vacuum bonds according to

$$E_{\mathrm{scaled}} = E_{\mathrm{vac}} - E_{\mathrm{vac}}\frac{E^{\mathrm{moth}}}{E^{\mathrm{cryst}}} \qquad (3)$$

where the interaction energy between the growth units in the bulk crystal $E^{\mathrm{cryst}} = E^{\mathrm{moth}} + E^{\mathrm{diss}}$ and E^{diss} is set equal to the dissolution enthalpy. Thus, the strongest interaction which was not included in the crystal graph equals −0.52 kT at 300 K after scaling. The resulting crystal graph is shown in Figure 2. Table 3 gives all interactions in the crystal graph before and after scaling. Since the crystal structure has a pseudo-6-fold symmetry whereas the real spacegroup is $P2_1$, many bonds are pseudo-symmetry-related resulting in sets of three, such as bonds c, d, and f and bonds a, e and g.

Growth Rates

The growth rates were determined by Monte Carlo simulations for all orientations parallel to a connected net. These orientations were determined using the program FACELIFT.[15] FACELIFT searches for periodic bond chains and combines these into connected nets. This resulted in 35 connected faces on both top sides and six side faces. Since the spacegroup does not contain an inversion center and the unique axis is along the needle direction, opposite top faces are not symmetry related. In contrast, the opposite side faces are related via the 2-fold axis. FACELIFT does not make a distinction between opposite faces and thus adds an inversion center to the morphology. We however performed separate Monte Carlo simulations for opposite top faces.

Figure 3 shows the growth rates as a function of the driving force for a representative set of all connected surfaces as obtained by Monte Carlo simulations. The solid lines represent the top faces (hkl) with a positive k-value, the dashed lines represent the opposite top faces, and the dash-dotted lines represent the side faces.

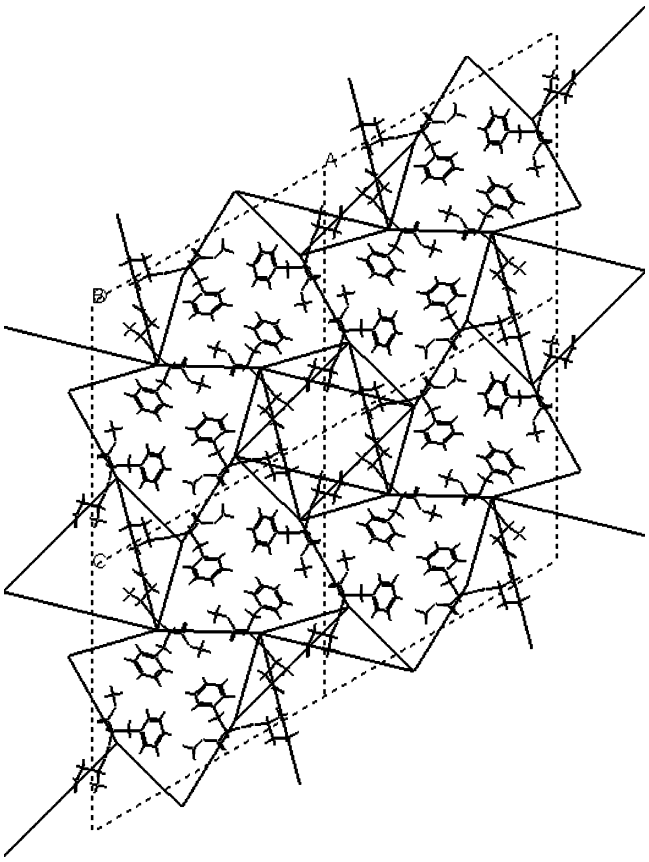

Figure 2. Four unit cells and the crystal graph of aspartame I-A after minimization including the water molecules, projected along [010]; the water molecules are not drawn.

Table 3. Crystal Graph[a]

label	bond GU−GU	direction [uvw]	length (Å)	bond energy	bond energy after scaling
a	1-6	[000]	9.30	−196.56	−26.95
b	1-2	[$\bar{1}$00]	8.93	−101.25	−13.89
c	1-1	[0$\bar{1}$0]	5.15	−93.51	−12.80
d	2-2	[0$\bar{1}$0]	5.15	−78.32	−10.75
e	2-3	[01$\bar{1}$]	10.80	−77.61	−10.63
f	3-3	[0$\bar{1}$0]	5.15	−74.85	−10.25
g	1-2	[$\bar{1}$10]	10.28	−67.15	−9.20
h	2-6	[100]	15.10	−27.95	−3.85
i	3-6	[001]	7.54	−20.17	−2.76
j	1-4	[000]	8.12	−15.98	−2.18
k	2-5	[100]	8.94	−14.31	−1.97

[a] The first GU is always in unit cell [000]. Bond energies in kJ/mol.

The figure shows that all faces have at least a small nucleation barrier. This is in contrast with the II-A form for which all top faces except one have a zero nucleation barrier. This difference is probably due to the reduced symmetry of the I-A form as compared to II-A. In this case, bonds do not completely cancel each other. To show the effect of the (broken) symmetry, we performed the Monte Carlo simulations using the crystal graph of aspartame I-A obtained after minimizing the structure without water molecules present. The results are given in Figure 4a. (The previously discussed graph was optimized with water, but the crystal graph did not contain water molecules.) This new graph is much more symmetric than the old graph and is only shown here to illustrate the effect of symmetry on the nucleation barrier. It is not a correct representation of the real

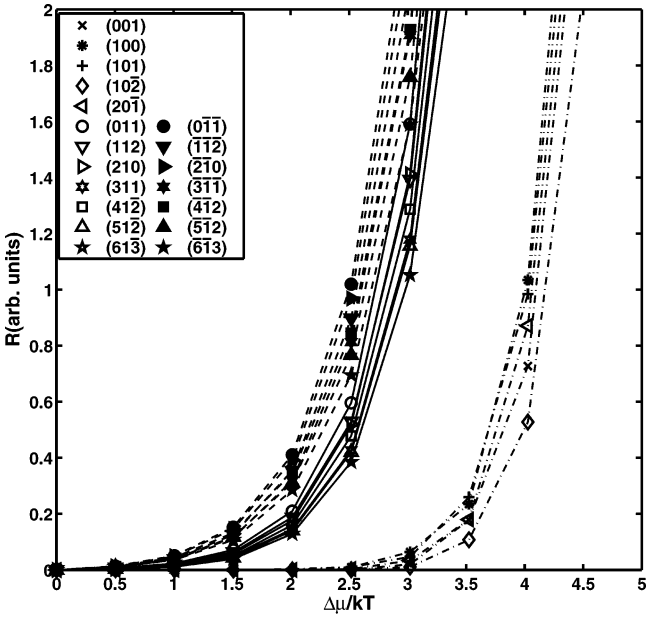

Figure 3. The growth rate as a function of the driving force for a representative set of all connected surfaces as obtained by Monte Carlo simulations. The solid lines and open markers represent the faces (*hkl*) with a positive *k*-value, the dashed lines and the full markers represent the negative *k* top faces and the dash−dotted lines represent the side faces.

aspartame structure. The corresponding growth rate plots, given in Figure 4b, show indeed no nucleation barrier for the top faces. Because of the higher symmetry, step energies that consist of differences in energy are smaller.

Figure 5 shows the experimental growth rates as a function of the growth temperature. The crystals were grown from aqueous solutions with different saturation temperatures of 40, 50, 60 and 70 °C. The growth rates in two directions were measured: in the needle direction (full markers) and perpendicular (open markers). The growth rate shows a nucleation barrier for both directions and at all saturation temperatures. The Monte Carlo simulation results presented in Figure 3 are in qualitative agreement with these observations.

Generally, two growth regimes can be observed: at low driving force slow growth and at high driving force rough linear growth. The critical undercooling, which indicates the transition between the two growth regimes, is for the needle direction much lower than for the side faces. For the side faces, this transition is only observed for the crystals grown from the solution with a saturation temperature of 60 °C. For all other solutions, growth of the side faces is hardly observed.

Apart from the qualitative agreement between the experimental results and the simulations, the driving forces at which the side faces start to grow in the experiment are for some of the experiments clearly lower than predicted. This cannot be explained by a spiral growth mechanism as the thin needles do not allow for spirals to develop. Aspartame crystals sometimes increase in thickness by tubular shafts that grow relatively fast along their side faces, the nucleation mechanism for these being unclear.

Morphology

Both the experimental and the Monte Carlo growth rate plots show that the side faces grow much more slowly than the top faces. This leads to a needlelike morphology. The experimental morphologies can be classified into five types depending on the degree of driving force. Spherulites consisting of needlelike crystals with a faceted form were observed at a driving force below $\Delta\mu = 0.20kT$ as is shown in Figure 6a,b. When the driving force exceeds $\Delta\mu \approx 0.20kT$, the tip of the needle splits and thus the needles become branched and curled (Figure 6c). Fibrous crystals were formed at driving forces between $\Delta\mu = 0.26kT$ and $0.32kT$.

As for the predicted morphology, Figure 7 shows two morphologies at two different driving forces obtained from Figure 3. In this figure, the faces are indexed. At

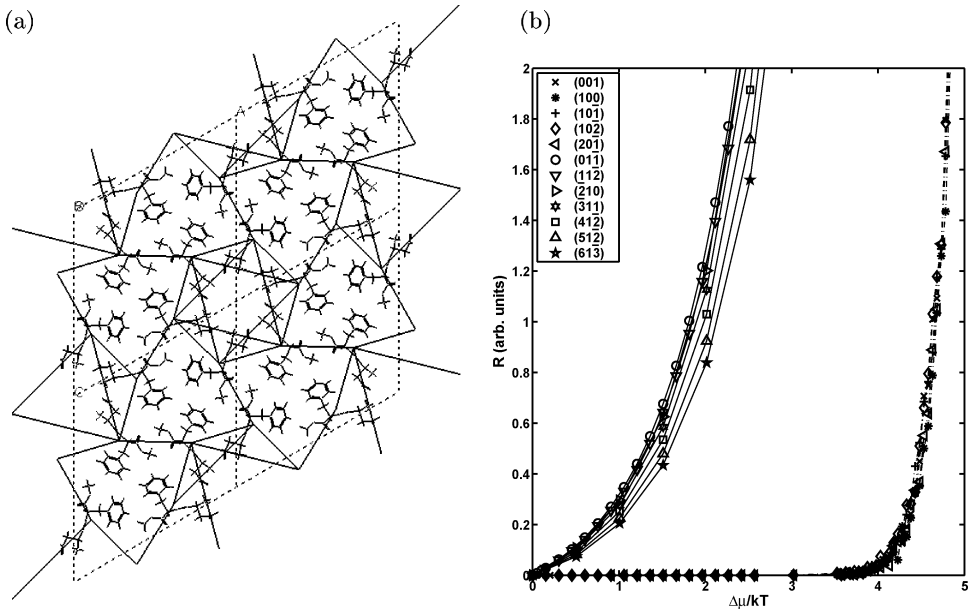

Figure 4. (a) The crystal graph obtained after minimizing the structure without water molecules. (b) The corresponding growth rate curves as a function of the driving force. The higher symmetry of the crystal graph lowers the nucleation barrier of the top faces.

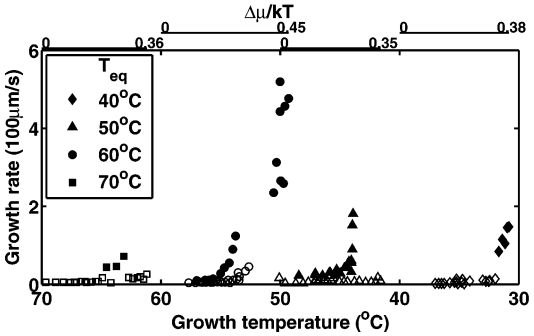

Figure 5. The experimental growth rates of aspartame form I-A measured in the needle direction (full markers) and the perpendicular direction (open markers) as a function of the growth temperature and the driving force (top scale). The crystals were grown from four aqueous solutions with different saturation temperatures of 40, 50, 60, and 70 °C.

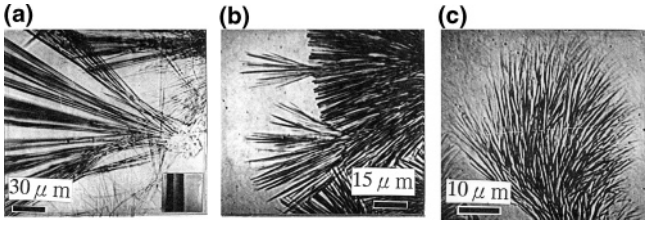

Figure 6. Spherulites of aspartame as a function of the driving force for a solution saturated at 40 °C. (a) $\Delta\mu \approx 0.07kT$, needles with faceted side faces, (b) $\Delta\mu \approx 0.11kT$, with partly faceted side faces, and (c) $\Delta\mu \approx 0.20kT$, without faceted side faces and curled tops.

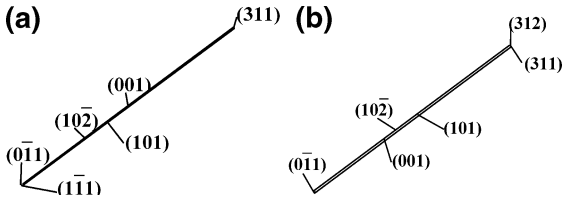

Figure 7. Two morphologies of aspartame I-A as obtained by the Monte Carlo simulations presented in Figure 3 at (a) $\Delta\mu = 2.5kT$ and (b) $\Delta\mu = 3kT$.

these driving forces, the top faces are however kinetically rough and therefore rounded. Although form I-A has a finite nucleation barrier for the top faces, the aspect ratio of the morphology is even larger than found for II-A.

Polarity

In the Monte Carlo simulations, the growth rates of the negative top faces are larger than for the positive top as can be seen in Figure 3. Comparing the opposite faces roughly results in a factor of 2 difference. This is why the morphologies in Figure 7 show different faces on the opposite top sides. Figure 8 shows a projection of the aspartame structure along the *c*-axis and indicates the slow and fast growing directions of the needle.

Experiments of growing crystals in water confirm this polar growth behavior. Figure 9 shows a difference image of two in situ images of a growing crystal with a time interval of approximately 1 s. L1 and L2 in the figure are the corresponding lengths of the needle crystal. The driving force was approximately 17%, and

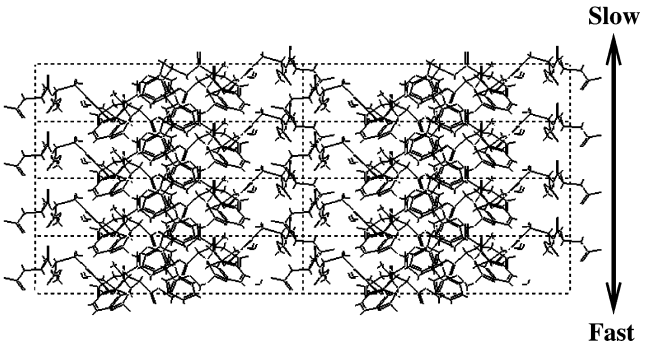

Figure 8. *c*-projection of eight unit cells of aspartame I-A. The arrows indicate the slow and fast growing needle directions.

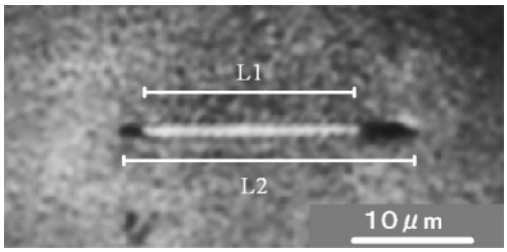

Figure 9. The difference image of two in situ images of a growing crystal with a time interval of approximately 1 s. L1 and L2 in the figure are the corresponding lengths of the needle crystal. The driving force was approximately 17%, and the saturation temperature of the solution was 60 °C.

the saturation temperature of the solution was 60 °C. It can be clearly seen that the gained length on one end of the needle is much larger than on the other end. This difference is roughly a factor of 2, in correspondence with the Monte Carlo results. The orientation of the molecules in the needle crystal of Figure 9 is however not known.

Note that the polarity found in the Monte Carlo simulations is due to the structural difference between the opposite faces and is not caused by a solvent effect, since the solvent is not included in the Monte Carlo simulations. A forthcoming paper will discuss the cause of this polarity in detail.

Conclusions

In the present paper, we present structural, morphological, and growth rate data for aspartame form I-A and compare the latter with data obtained by Monte Carlo simulations. The Monte Carlo simulations result in the same morphology as observed experimentally and also the correct polarity in growth rate was obtained.

This structure of form I-A has a lower spacegroup symmetry than does form II-A. For form II-A, some of the top faces have step energies that are zero because symmetry-related interactions in the crystal graph cancel each other. For the present structure, this is not the case since these interactions are now not symmetry-related anymore. The pseudo-6-fold symmetry however makes these interactions similar resulting in step energies small enough to obtain a needle morphology. For a graph with a higher symmetry as a result of neglecting the water molecules, higher growth rates of the top faces were found due to even lower step energies.

Although the morphology and the general growth behavior were correctly reproduced by the simulations, the range in the relevant driving force was too high. The interactions in the crystal graph were scaled such that the total crystallization energy is the same as in the experiments. Nevertheless, the driving force at which the faces start to grow is much higher than in the experiments. Although it is appealing to explain this difference by the presence of a spiral growth mechanism, this can be ruled out because of the extremely thin crystal morphology.

Acknowledgment. H. M. C. would like to thank the Council for Chemical Sciences of The Netherlands Organisation for Scientific Research (CW-NWO) for financial support. K. T. would like to acknowledge Ajinomoto Co. Ltd. for the supply of the aspartame and discussions on the growth method of the crystals.

References

(1) Allen, F. H. The Cambridge Structural Database: a quarter of a million crystal structures and rising. *Acta Crystallogr. B.* **2002**, *58*, 380−388.

(2) Cuppen, H. M.; van Eerd, A. R. T.; Meekes, H. Needlelike morphology of aspartame. *Cryst. Growth Des.* **2004**, *4*, 989−997.

(3) Meguro, T.; Kashiwagi, T.; Satow, Y. Crystal structure of the low-humidity form of aspartame sweetener. *J. Pept. Res.* **2000**, *56*, 97−104.

(4) North, A. C. T.; Phillips, D. C.; Mathews, F. S. A semi-empirical method of absorption correction. *Acta Crystallogr. A* **1968**, *24*, 351−359.

(5) Beurskens, P. T.; Beurskens, G.; Bosman, W. P.; de Gelder, R.; Garcia-Granda, S.; Gould, R. O.; Israel, R.; Smits, J. M. M. *DIRDIF-96*; A computer program system for crystal structure determination by Patterson methods and direct methods applied to difference structure factors; Crystallography Laboratory: University of Nijmegen, The Netherlands, 1996; http://www.crystallography.nl.

(6) Hatada, M.; Jancarik, J.; Graves, B.; Kim, S.-H. Crystal structure of aspartame, a peptide sweetener. *J. Am. Chem. Soc.* **1985**, *107*, 4279−4282.

(7) Sheldrick, G. M. *SHELXL97*, program for the refinement of crystal structures, University of Göttingen, Germany, 1997.

(8) Boerrigter, S. X. M.; Josten, G. P. H.; van de Streek, J.; Hollander, F. F. A.; Los, J.; Cuppen, H. M.; Bennema, P.; Meekes, H. MONTY: Monte Carlo crystal growth on any crystal structure in any crystallographic orientation; application to fats. *J. Phys. Chem. A* **2004**, *108*, 5894−5902.

(9) Gilmer, G. H.; Bennema, P. Simulation of crystal growth with surface diffusion. *J. Appl. Phys.* **1972**, *43*, 1347−1360.

(10) van der Eerden, J. P. Crystal growth mechanisms. In *Handbook of Crystal Growth*; Hurle, D. T. J., Ed.; Elsevier: Amsterdam, 1993; Vol. 1a, Chapter 5, p 307.

(11) Grimbergen, R. F. P.; Meekes, H.; Bennema, P.; Strom, C. S.; Vogels, L. J. P. On the Prediction of Crystal Morphology. I. The Hartman-Perdok Theory Revisited. *Acta Crystallogr., Sect. A* **1998**, *54*, 491−500.

(12) Sugiyama, K.; Ozawa, T.; Nagashima, N.; Uchida, Y. Dipeptide crystals, a process for their production, tablets containing the dipeptide crystals and a process for the production thereof. European Patent EP0119837, 1984.

(13) *Cerius*^{2} *User Guide*; Accelrys Inc.: San Diego, CA, 1997.

(14) Grimbergen, R. F. P. DSM Composite Resins, Zwolle, The Netherlands. Private communication, 2003.

(15) Boerrigter, S. X. M.; Grimbergen, R. F. P.; Meekes, H. *FACELIFT-2.50*; a program for connected net analysis; Department of Solid State Chemistry, University of Nijmegen, The Netherlands, Feb 2001; Hugo.Meekes@science.ru.nl.

CG049676M